Weak hysteresis in a simplified model of the L-H transition

M. A. Malkov and P. H. Diamond
Center for Astrophysics and Space Sciences and Department of Physics, University of California, San Diego, La Jolla, California 92093-0424, USA

(Received 19 September 2008; accepted 9 December 2008; published online 20 January 2009)

A simple one-field L-H transition model is studied in detail, analytically and numerically. The dynamical system consists of three equations coupling the drift wave turbulence level, zonal flow speed, and the pressure gradient. The fourth component, i.e., the mean shear velocity, is slaved to the pressure gradient. Bursting behavior, characteristic for predator-prey models of the drift wave - zonal flow interaction, is recovered near the transition to the quiescent H-mode (QH) and occurs as strongly nonlinear relaxation oscillations. The latter, in turn, arise as a result of Hopf bifurcation (limit cycle) of an intermediate fixed point (between the L- and H-modes). The system is shown to remain at the QH-mode fixed point even after the heating rate is decreased below the bifurcation point (i.e., hysteresis, subcritical bifurcation), but the basin of attraction of the QH-mode shrinks rapidly with decreasing power. This suggests that the hysteresis in the H-L transition may be less than that expected from S-curve models. Nevertheless, it is demonstrated that by shaping the heating rate temporal profile, one can reduce the average power required for the transition to the QH-mode. © *2009 American Institute of Physics*. [DOI: 10.1063/1.3062834]

I. INTRODUCTION

The high confinement regime (H-mode) discovered by the ASDEX team[1] a quarter-century ago is widely regarded as a fundamental breakthrough in magnetic confinement physics. Yet, the transition mechanism from the low (L) to high (H) confinement mode is not fully understood.[2–6] There are transport models, which are instrumental in furthering our understanding of the transition. However, because of the complexity of transition phenomenon, they tend to be increasingly, if not excessively, detailed.[7–13] Therefore, there is high demand for a simple, illustrative *theoretical* model with a minimal number of *critical* quantities responsible for the transition. Such models usually yield or encapsulate basic insight into complicated phenomena. Some obvious practical questions are: Does an observed transition occur at the minimum power or it can be reduced by adjusting other parameters, or can the power be reduced after the transition to H-mode? Understanding of the character of bifurcation (e.g., sub- versus supercritical, etc.) and hysteresis (if present) is required for the answer. In the quest of such simple physical models, there are two avenues to explore.

One avenue is to develop a preferably one-dimensional (1-D) evolutionary model with a minimal set of variables. Since such models are often still complicated, one is forced to turn to steady state solutions. Also, some of the variables are not described self-consistently or obtained only numerically. All these shortcomings obscure the essence of L-H transition phenomenon. Under these circumstances a second, complementary approach based on zero-dimensional (0-D; i.e., spatially averaged, Galerkin-type) models becomes useful (see, e.g., Refs. 14 and 15). The 0-D models may be reduced by a projection technique from the 1-D continuous media models or from their more general prototypes. The advantage of 0-D models is that the dynamics of L-H transition can be studied using powerful tools of the bifurcation theory of dynamical systems. It is this second approach that this paper pursues.

The most likely mechanism behind the L-H transition is an $\mathbf{E}\times\mathbf{B}$ shearing of turbulent eddies (drift wave, DW) that actually drive the transport.[16–24] The $\mathbf{E}\times\mathbf{B}$ shear flow comes in two flavors. One flavor is the mean flow in which the radial electric field E_r and thus the plasma poloidal velocity change smoothly in r and are nearly stationary. The other is the zonal flow (ZF) with a radially irregular behavior varying slowly in time. An important difference between the two is that the mean flow does not need to be sustained by DW turbulence and thus can shear the DWs to zero, while the second one (ZF) is fed on the DW turbulence and decays via collisions if the DWs vanish. This suggests that both the mean flow and the zonal flow must act in concert with each other, suppressing the DW turbulence and transport. Clearly, the primary driver of the DW turbulence, i.e., the pressure or density gradient, must also be included to close the feedback loop. Such a line of arguments led the authors of Refs. 25 and 26 to develop a minimalistic 0-D model where the DW turbulence, both the mean and zonal flows, and the driving pressure gradient are included. A slowly increasing heat source powers the pressure gradient to let the system evolve from the L-mode through a transient oscillatory behavior into the quiescent H-mode. In the latter regime, neither DW nor ZF survives and only the mean flow persists, supporting an enhanced pressure gradient. Thus, an intermediate, oscillatory mode has been reproduced and its possible relation to the dithering observed in many experiments[27] prior to the establishing of H-mode has been discussed. Note that a third-order model that does not distinguish between the zonal and the mean flows was suggested earlier in Ref. 28.

The purpose of the present paper is to study all possible

stationary regimes including the intermediate mode, their stability, and transition dynamics. Specifically, the following questions will be addressed:

(1) stability of stationary regimes, their classification depending on physical parameters;
(2) classification of transitions (character of bifurcations, role of initial conditions), critical role of the zonal flow;
(3) power up/down asymmetry, the depth of hysteresis;
(4) structure and dimensionality of the phase space where an essential dynamics occur (center manifolds);
(5) role and physical cause of nonlinear oscillations preceding the transition (dithering), extent of the dithering above the transition threshold.

It should be noted that the L-H transition through the dithering phase is still difficult to describe within the continuous media type models mentioned above.[29–31] Although those models do reproduce bursting, the pressure gradient has been included, only not self-consistently (as opposed to the present 0-D model), in the form of a fixed DW growth rate. The bursting results from the interplay between the DW and ZF turbulence (predator-prey type dynamics). The fixed DW growth rate means that the "prey's" living resources are fixed. It is thus logical to start with an extension of a 0-D model to a higher level by describing the transition phase with a self-consistent evolution of the mean pressure gradient and the mean flow.[25,26]

In the next section, we first demonstrate the necessity of such an extension by considering limitations of a simplest two ordinary differential equation (2-ODE) model with a fixed pressure gradient (DW instability growth rate). We also develop a more complicated 3-ODE model introduced in Refs. 25 and 26 by analyzing its fixed points and other invariant manifolds. In Sec. III we consider the stability of those invariant manifolds setting a stage for studying various transition scenarios in Sec. IV. We summarize and discuss the results in Sec. V.

II. ZERO-DIMENSIONAL MODELS FOR LH TRANSITIONS

A. A simple 2-ODE Lotka–Volterra model

There exists an extensive literature on ODE models of the L-H transition. Most of them are 3-ODE autonomous or time-dependent systems (typically with a variable heating rate). One such system will also be the subject of the present paper. However, to make contact with the fundamental ideas that are behind the low-dimensional dynamical systems, we start with a simplest 2-ODE model. One of the first such models was suggested in Ref. 32 (see also Ref. 33). It describes the evolution of temperature fluctuations and the shear flow. It can be transformed into the following dimensionless systems with only one parameter:

$$\frac{d\Omega}{dt} = (T-\mu)\Omega, \tag{1}$$

$$\frac{dT}{dt} = (1-\Omega)T. \tag{2}$$

Here the variable Ω represents a square of properly normalized shearing rate and T represents the square of temperature fluctuation level. The growth rate of the thermal instability is normalized to unity (as seen from the second equation), while the viscous damping of the flow is represented by the only parameter of the system: μ. The system of Eqs. (1) and (2) is a familiar Lotka–Volterra system emphasizing ecological resemblance of many popular L-H transition models of a "predator-prey" family. Here the shearing rate Ω is a predator with a natural death rate μ living on the prey T with a unity reproduction rate. The system can be written in the form

$$\frac{d\Omega}{dT} = \frac{1-\mu/T}{1/\Omega - 1}, \tag{3}$$

where it shows an obvious first integral

$$T + \Omega - \ln(\Omega T^{\mu}) = \text{const}. \tag{4}$$

This reveals the phase portrait of the system completely. There is a hyperbolic singular point at $\Omega=T=0$ (L-mode) with one stable $(T=0,\Omega>0)$ and one unstable $(\Omega=0, T>0)$ invariant manifold. The second singular point is a center at $\Omega=1$, $T=\mu$ (H-mode), so that the rest of the phase plane $(\Omega,T>0)$ is covered by closed orbits around this point. Obviously, the system by itself does not make any L-H or H-L transition for that reason. Note that since Eqs. (1) and (2) possess the above integral, they can easily be rewritten in a Hamiltonian form, using the variables $\xi=\ln\Omega$ and $\eta=\ln T$ with the Hamiltonian $H=\exp(\xi)+\exp(\eta)-\xi-\mu\eta$.[34] However, we use a different formalism below.

In general, the dynamics of this system is a trivial rotation around the H-mode, which can be most efficiently described by transforming Eqs. (1) and (2) to the Poincaré normal form. This can be conveniently done by introducing a complex variable z instead of Ω and T. The new variable z characterizes the deviation from the H-mode singular point:

$$z = \sqrt{\mu}(\Omega-1) + i(T-\mu). \tag{5}$$

For z, we have the following equation that can be derived from the system (1) and (2):

$$\frac{dz}{dt} = -i\sqrt{\mu}z - \kappa(z^2 - \bar{z}^2). \tag{6}$$

Here, $\bar{z}$ denotes a complex conjugate (c.c.) of z and $\kappa=i/4+1/4\sqrt{\mu}$.. The first step to the Poincaré normal form is to remove the quadratic terms from Eq. (6) by transforming $z\mapsto w$:

$$z = w - \frac{i\kappa}{\sqrt{\mu}}\left(w^2 + \frac{1}{3}\bar{w}^2\right). \tag{7}$$

Using this new variable, Eq. (6) can be rewritten as

$$\frac{dw}{dt} = -i\sqrt{\mu}w + \frac{2i\kappa}{\sqrt{\mu}}\left[w^2\left(\kappa w + \frac{\bar{\kappa}}{3}\bar{w}\right) + \text{c.c.}\right]. \tag{8}$$

Transforming to yet a new variable $w\mapsto u$, introduced by

$$w = u + \frac{1}{\mu}\left(\frac{|\kappa|^2}{2}\bar{u}^3 + \frac{\kappa^2}{3}|u|^2\bar{u} - \kappa^2 u^3\right), \tag{9}$$

we finally obtain the Poincaré normal form

$$\frac{du}{dt} = -i\sqrt{\mu}u\left(1 - \frac{1+\mu}{24\mu^2}|u|^2\right). \tag{10}$$

Since $|u|=$const is an integral of motion, the system dynamics is a simple circular motion around the origin $u=0$ with the following angular frequency:

$$\omega = \sqrt{\mu}\left(1 - \frac{1+\mu}{24\mu^2}|u|^2\right). \tag{11}$$

With increasing amplitude $|u|$, the frequency decreases to zero when the trajectory reaches the second fixed point (L-mode).

As we have already mentioned, this system does not intrinsically describe any L-H transition, but merely the oscillations around the H-mode fixed point, which in the limit of $\omega \to 0$ become strongly nonlinear reaching the L-mode fixed point. Of course, since this system is structurally unstable, it may be easily modified in such a way that the center at the H-mode will become a stable or unstable focus and both fixed points may become connected (or a limit cycle may be formed). However, the question arises as to whether the description of the L-H transition phenomenon by modifying a structurally unstable dynamical system is justified and whether a structurally stable dynamical system with an intrinsic transition is preferable. We believe that the last question should be answered in the affirmative. The spontaneous character of L-H transitions has been repeatedly observed in experiments.[18]

There are a number of models in the literature that exhibit a spontaneous L-H transition when parameters are set close to their critical values. These models are more complicated than the system considered above, yet they allow a comprehensive analysis. They have more variables (typically 3-ODE systems and more; see, e.g., Refs. 14, 28, 31, and 35–39) and often a large number of parameters. Clearly, the model selection criteria, apart from the sound physics behind them, should be based on their capability to reproduce key experimental facts such as spontaneous L-H transitions, characteristic intermediate regimes (such as dithering), or hysteresis. In the next section we consider one recent model of this kind.

B. 3-ODE system

The L-H transition model formulated in Refs. 25 and 26 operates on the following four quantities: (i) drift wave turbulence level $\mathcal{E}$, (ii) drift wave driving temperature gradient $\mathcal{N}$, (iii) zonal flow velocity V_{ZF}, and (iv) mean flow shear V. Note that the latter quantity is slaved to the temperature gradient, $V=d\mathcal{N}^2$, where d is a constant, so that the system is actually of the third order (3-ODE). The dynamical system was originally introduced in the following form[25]

$$\frac{d\mathcal{E}}{d\tau} = (\mathcal{N} - a_1\mathcal{E} - a_2 d^2\mathcal{N}^4 - a_3 V_{\mathrm{ZF}}^2)\mathcal{E}, \tag{12}$$

$$\frac{dV_{\mathrm{ZF}}}{d\tau} = \left(\frac{b_1\mathcal{E}}{1 + b_2 d^2\mathcal{N}^4} - b_3\right)V_{\mathrm{ZF}}, \tag{13}$$

$$\frac{d\mathcal{N}}{d\tau} = -(c_1\mathcal{E} + c_2)\mathcal{N} + q(\tau). \tag{14}$$

Apart from the driver $q(\tau)$ in Eq. (14) (heat source), which will play a role of the main control parameter in our studies of different equilibria of the system, this system has as many as nine other parameters; e.g., a_i, b_i, c_i, and d. These parameters and various terms have the following meanings. The first term on the right hand side (r.h.s.) of Eq. (12) represents the drift wave instability driven by the pressure gradient. The instability has a scaled growth rate $\mathcal{N}$. The other terms are: nonlinear saturation with the coefficient a_1 and suppression of DW by the mean and zonal flow (coefficients a_2 and a_3). The first term on the r.h.s. of Eq. (13) describes the ZF generation by the Reynolds stress in the DW turbulence (b_1, with the suppression effect from the mean flow b_2). The physical meaning of this suppression effect is the refraction of the DWs in a sheared mean flow, which is also present in Eq. (12). The second term on the r.h.s. of Eq. (13) corresponds to the linear (collisional) damping of ZF (b_3). Equation (14) describes the relaxation of the pressure gradient $\mathcal{N}$ due to the turbulent diffusion (the first term on the r.h.s., coefficient c_1) and the neoclassical transport c_2.

A detailed explanation and derivation of various terms in Eqs. (12)–(14) can be found in Ref. 40 (see also Refs. 3, 6, 34, and 38 for more recent and more general discussions). We merely note here that Bian and Garcia[34] associate the turbulent transport term with the convective transport of the pressure. Since both interpretations result in the same (quadratic) dependence of the transport term on the fluctuation amplitude, most probably they are indistinguishable within 0-D models. A related question is that of whether the electric field shear reduction of particle and heat fluxes can be adequately accounted for within such models. Since the reduction leads to the formation of transport barriers, it can hardly be included into these models without re-deriving them from nonlocal standpoint.

To start, we note that the number of parameters in Eqs. (12)–(14) can be reduced to five by rescaling the variables and time. First of all, one can set $d=1$ since d can be absorbed into a_2 and b_2. After introducing the following rescaled variables, and time t,

$$N = a_2^{1/3}\mathcal{N}, \quad E = a_1 a_2^{1/3}\mathcal{E}, \quad U = a_2^{1/3}a_3 V_{\mathrm{ZF}}^2, \quad t = a_2^{1/3}\tau,$$

along with a new set of parameters

$$\vartheta = \frac{2b_1}{a_1 a_2^{2/3}}, \quad \rho = \frac{c_2}{a_2^{1/3}}, \quad \sigma = \frac{c_1}{a_1 a_2^{2/3}},$$

$$\zeta = \frac{b_2}{a_2^{4/3}}, \quad \eta = \frac{b_3}{b_1}a_1 a_2^{1/3},$$

the system of equations (12)–(14) can be rewritten as

$$\frac{dE}{dt} = (N - N^4 - E - U)E, \tag{15}$$

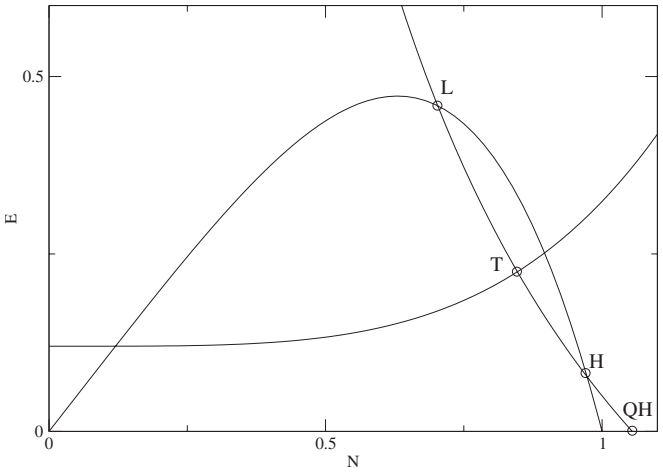

FIG. 1. Singular points of the dynamical system given by Eqs. (15)–(17). The equilibria are shown as the intersection points of the three curves, each of which nils one of the three right hand sides of the system in the $U=0$ projection. The curve connecting the origin with $N=1$ is given by $E=N(1-N^3)$, the rising curve is given by $E=\eta(1+\zeta N^4)$, while the falling curve is from the heat balance $N=q(\rho+\sigma E)^{-1}$. The latter also intersects the $E=0$ axis at the stable equilibrium point QH (see text). The parameters are $\vartheta=19$, $\eta=0.12$, $\rho=0.55$, $\sigma=0.6$, $\zeta=1.7$, and $q=0.58$.

$$\frac{dU}{dt}=\vartheta\left(\frac{E}{1+\zeta N^4}-\eta\right)U, \tag{16}$$

$$\frac{dN}{dt}=q(t)-(\rho+\sigma E)N. \tag{17}$$

It is worthwhile to summarize here the important features of this dynamical system. Note that some of them were identified in Refs. 25 and 26. Depending on the parameters, the system given by Eqs. (15)–(17) has up to the four fixed points, as illustrated in Fig. 1 using a $N-E$ projection. With increasing q, the system typically (but not for all values of other parameters and initial conditions) evolves from what we call an L-mode to a transient (intermediate) oscillatory T-mode, then to H-mode and finally to a quiescent H-mode (or QH-mode).

- the L-mode is characterized by

$$U=0,\qquad E=E_L\equiv N_L(1-N_L^3)>0, \tag{18}$$

where N_L is the smaller of the two positive roots of the equation

$$N^2(1-N^3)+\frac{\rho}{\sigma}N=\frac{q}{\sigma}. \tag{19}$$

Here, q is assumed to be constant or slowly varying in time.

- The transient mode fixed point (T-mode) can be conveniently described by the following sequence of relations:

$$E_T=\eta(1+\zeta N_T^4), \tag{20}$$

$$U_T=N_T(1-N_T^3)-E_T, \tag{21}$$

$$N_T=\frac{q}{\rho+\sigma E_T}. \tag{22}$$

- The H-mode is given by $E_H\equiv N_H(1-N_H^3)$, where N_H is the larger root of Eq. (19).
- Quiescent H-mode (QH-mode) establishes when the heat balance curve [Eq. (22)] intersects the N axis ($E=U=0$). Obviously, $N_{QH}=q/\rho$ at this fixed point [Eqs. (15) and (16)].

Note that the L- and H-modes share the property $U=0$, but $E\neq 0$. The T-mode is characterized by both $E\neq 0$ and $U\neq 0$, while in the QH-mode, $U=E=0$. For both H- and QH-modes to exist, it is necessary that $N_{\mathrm{QH}}=q/\rho>1$, which is also the stability condition for the QH-mode.

Figure 1 shows the arrangement of the fixed points for one particular set of parameters when all the fixed points of the system exist. Clearly, some of the fixed points may disappear while parameters change. For example, the H-mode obviously fails to exist when QH-mode on the N axis goes below unity. As we noted, for the H-mode to exist, it is necessary that $q/\rho>1$. Note that if the latter is not the case, then also the QH mode is unstable, according to Eq. (15). On the other hand, for H- and L-modes to coexist, the heating parameter should not exceed a limit $q_{\max}$, $1<q/\rho<q_{\max}/\rho$. It can be obtained by assuming that the curves given by Eqs. (21) and (22) touch each other and the L- and H-modes merge into one. The value of pressure gradient at this point is determined by

$$N=\frac{2}{3\sigma}\left(\sqrt{\rho^2+\frac{15}{4}\sigma q}-\rho\right).$$

The exact analytic expression for $q_{\max}$ is cumbersome and we do not reproduce it here. A simple upper bound to q, which can be obtained from the requirement $N<1$, is $q<(4\rho+3\sigma)/5$.

As it was already mentioned, we consider q as the main control parameter and we generally follow the bifurcation sequence as q increases. Note that Refs. 25 and 26 studied the bifurcation of the system given by Eqs. (12)–(14) by making $q(t)$ slowly growing in time from zero to some final value sufficient to reach the QH-mode in each run, so that all the transitions occur consequently on much shorter time scales. Here we study the reduced system given by Eqs. (15)–(17) using two different approaches. The first approach is to treat q as a fixed control parameter and look for the fixed points and limit cycles that may branch off from some of these fixed points. In particular, we study the Hopf bifurcation of the T-mode equilibrium into a limit cycle on a center manifold of the system. The center manifold here is a two-dimensional attractor of our three-dimensional system formed by eigenspace spanned on the two purely imaginary complex conjugated eigenvalues. The third eigenvalue has $\mathrm{Re}\,\lambda<0$, which ensures local attraction to the center manifold. We also consider stability of equilibria and the transition from the limit cycle to a next equilibrium. This elucidates conditions under which the transitions to higher modes

such as, e.g., L→T, T→H, or T→QH occur. Special attention is paid to the reverse transition and to the question of hysteresis.

The second approach aims at testing the possibility of reaching one of the H-mode fixed points at lower values of average power input $\langle q(t)\rangle$ by choosing properly modulated heating rate $q(t)$, which makes the fixed point a stable attractor. This resembles the stabilization of an inverted pendulum by applying an oscillating force. A ramification of this approach is to study power up/down asymmetry in order to better understand the character of hysteresis.

III. STABILITY OF THE FIXED POINTS

The first simple result about the stability of the fixed points described in the previous section relates to the $U=0$ (no ZF) manifold. The fixed points are the L- and H-modes, and the QH-mode which, however, also requires $E=0$ (no DWs). The stability of the QH-mode is obviously guaranteed by the condition $N>1$, or by

$$q/\rho > 1. \tag{23}$$

The sufficient condition for the stability of the $U=0$ manifold in general follows from the consideration of a function

$$V(N) = N - (1+\zeta\eta)N^4 - \eta \tag{24}$$

[see Eq. (16)]. In particular, if $V(N_{\max})<0$, where

$$N_{\max} = 4^{-1/3}(1+\zeta\eta)^{-1/3}$$

is the maximum point of $V(N)$, the manifold $U=0$ is stable. The stability condition can thus be written as

$$\eta(1+\zeta\eta)^{1/3} > 3/4^{4/3}. \tag{25}$$

Note that the stability condition of the $U=0$ manifold is independent of the control parameter q. The manifold $U=0$ is a *center manifold* of this system, and when the stability condition $V(N)<0$ is fulfilled, the dynamics is limited to this manifold and remains essentially two dimensional.

Having established the criterion for the system to remain on the $U=0$ manifold, we turn to the conditions under which the fixed points L and H may become unstable, under the constraint $U=0$; i.e., if the inequality (25) holds. Since both the L and H fixed points are determined by Eq. (19), we can use the same equations for L, H modes and write

$$E = E_{L,H} + E_1,$$

$$N = N_{L,H} + N_1.$$

Next, we linearize the system given by Eqs. (15) and (17) around these fixed points assuming $U\equiv 0$. The result can be written as one second-order equation for, e.g., N_1:

$$\frac{d^2N_1}{dt^2} + (E_{L,H} + \rho + \sigma E_{L,H})N_1 - E_{L,H} \times[\sigma N_{L,H}(4N_{L,H}^3 - 1) - \rho - \sigma E_{L,H}]N_1 = 0. \tag{26}$$

The instability condition can be obtained in a straightforward way and reads

$$N_{L,H}(5N_{L,H}^3 - 2) > \rho/\sigma.$$

Now, after differentiating the left hand side (l.h.s.) of Eq. (19) with respect to N, the above inequality becomes equivalent to the condition of choosing the larger root of Eq. (19); i.e., the one to the right of the maximum point of its l.h.s. Therefore, the instability condition can be fulfilled only for the H-mode. We thus draw the following conclusions about the routs to the improved confinement modes:

- Since the L-mode is stable on the $U=0$ manifold, any transition from L-mode to a higher confinement mode occurs by leaving the $U=0$ manifold; i.e., the zonal flow must be generated.
- Since the H-mode is a saddle point on the $U=0$ plane, the reverse (H→L) transition can occur on $U=0$ manifold.

These simple properties of the transition dynamics will be illustrated below.

Next, we consider the stability of the transient fixed point given by Eqs. (20)–(22). As opposed to the previous case the center manifold associated with this singular point of the system is not limited to any of the three coordinate planes in the (E,U,N) space. Nevertheless, as we shall see, there is one essentially negative eigenvalue at this fixed point so that there is a local manifold transversal to the corresponding eigenvector, to which all the trajectories rapidly attract and the further dynamics occur on this two-dimensional manifold. To study stability in this situation we linearize Eqs. (15)–(17) around the fixed point [which is given by Eqs. (20)–(22)] by representing E,U and N as follows:

$$E = E_T + E_1, \quad U = U_T + U_1, \quad N = N_T + N_1.$$

Here, E_1, U_1, and N_1 are assumed to be small. Rescaling time as $t'=E_T t$ for convenience, we obtain the following system of equations:

$$\frac{dE_1}{dt'} = -E_1 - U_1 - \beta N_1,$$

$$\frac{dU_1}{dt'} = \mu E_1 - \kappa N_1, \tag{27}$$

$$\frac{dN_1}{dt'} = -\gamma N_1 - \nu E_1.$$

In addition, we have introduced the following notations:

$$\mu = \frac{\vartheta U_T}{E_T(1+\zeta N_T^4)}, \quad \kappa = \frac{4\vartheta\zeta U_T N_T^3}{(1+\zeta N_T^4)^2},$$

$$\nu = \sigma N_T/E_T, \quad \gamma = \sigma + \rho/E_T \quad \beta = 4N_T^3 - 1.$$

The equation for the eigenvalues λ takes the form

$$\lambda^3 + (\gamma+1)\lambda^2 + (\gamma+\mu-\nu\beta)\lambda + \gamma\mu + \nu\kappa = 0. \tag{28}$$

Of the three roots of this equation, one is real and negative for the values of parameters of interest. We denote it by $\lambda_3<0$, while the two remaining $\lambda_{1,2}$ are complex and $\lambda_1=\bar{\lambda}_2$. As the control parameter q increases (with all the

other parameters fixed), the real parts $\mathrm{Re}\,\lambda_{1,2}$ cross zero at some critical value of $q=q_*$, and the system undergoes Hopf bifurcation to a limit cycle whose amplitude grows with $q-q_*>0$. For $q<q_*$ the fixed point is a stable focus.

To see how the loss of stability occurs at $q=q_*$, it is convenient to separate the stable eigenvalue λ_3 from $\lambda_{1,2}$. For, we use the following substitution:

$$\lambda = \frac{2}{\sqrt{3}}\sqrt{\frac{1}{3}(\gamma-\gamma^2-1)+\mu-\beta\nu\phi}-\frac{\gamma+1}{3}, \tag{29}$$

and work with ϕ rather than with λ. For ϕ, we obtain the following equation,

$$4\phi^3+3\phi+w=0, \tag{30}$$

where we have denoted

$$w=\frac{2\gamma^3+3(\gamma+1)(3\beta\nu-\gamma)+9\mu(2\gamma-1)+27\nu\kappa+2}{6\sqrt{3}\left[\frac{1}{3}(\gamma-\gamma^2-1)+\mu-\beta\nu\right]^{3/2}}. \tag{31}$$

From Eq. (30), we can express one of the roots ϕ_3 as

$$\phi_3=-\sinh\left(\tfrac{1}{3}\sinh^{-1}w\right),$$

so that λ_3 will be given by Eq. (29) with $\phi=\phi_3$. The other two roots can thus be expressed through ϕ_3 using the quadratic equation, which can be derived from Eq. (30):

$$\phi^2+\phi_3\phi+\phi_3^2+\tfrac{3}{4}=0.$$

The two remaining roots are

$$\phi_{1,2}=-\frac{1}{2}\phi_3\pm\frac{i\sqrt{3}}{2}\sqrt{1+\phi_3^2}.$$

Using Eq. (29) again, we obtain from the last equation the following criterion of instability of the transient fixed point:

$$\sqrt{3}\sqrt{\tfrac{1}{3}(\gamma-\gamma^2-1)+\mu-\beta\nu}\,\sinh\left(\tfrac{1}{3}\sinh^{-1}w\right)>\gamma+1. \tag{32}$$

Although the last condition is a general one, it is somewhat impractical due to the large number of parameters involved. However, in terms of the main control parameter q, it is locally equivalent to $q>q_*$.

IV. TRANSITION DYNAMICS

The location of singular points (Fig. 1) along with their stability analysis presented in the previous section helps to understand the transition dynamics. For sufficiently low q, only the L-mode is stable, which lies in the plane $U=0$ and is characterized by a finite level of the drift turbulence given by Eq. (18). As the control parameter q grows, so that E exceeds the critical level of the zonal flow stability

$$E_L \geqslant \eta(1+\zeta N_L^4),$$

the zonal flow is generated. The only stable point for this set of parameters is the transient oscillatory fixed point (stable focus), which, however is situated outside of the $U=0$ manifold [see Eqs. (20)–(22)] so that the system leaves the $U=0$ manifold and moves to the transient fixed point. However,

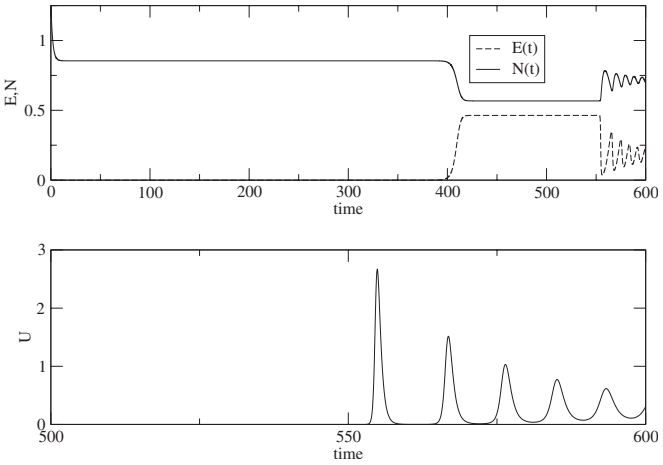

FIG. 2. Upper panel: Transition from H to L and then to the transient oscillatory (T) mode, which is stable focus for the given set of parameters, shown in variables N and E. The heating rate $q=0.47$; other parameters are fixed at the same values as in Fig. 1. The transition starts from the overpowered state near the H-mode and proceeds to the unstable H-mode, then to the unstable L-mode, and finally to the stable transient mode. Lower panel: Transition to the T-mode shown for U.

the dynamics is richer than that. In particular, as it is seen from the previous section, the H-mode corresponds to a saddle point on the $U=0$ plane so that it contains both stable and unstable invariant manifolds. The significance of this is demonstrated in Fig. 2, where the system undergoes a series of transitions for the fixed values of parameters. The solution starts from an overpowered state near H-mode which is unstable along with the QH-mode, since $q<q_{\mathrm{crit}}$. As we just mentioned, however, the H-mode fixed point has a stable manifold, so some trajectories are attracted to the H-mode, and stay there for a very long time ($t\simeq 400$, for the particular trajectory shown in Fig. 2). The system then makes a quick transition to the L-mode. Although the latter is also unstable for the given parameters, the above argument about the stable manifold of the saddle point applies as well so that the system stays in the L-mode for another 150 units of time. Thus, *both H- and L-modes constitute distinct metastable states* for the given values of parameters. Eventually, the system transits to the oscillatory stable state, which is the only stable fixed point in this case. Note that metastable states have been observed earlier by Hu and Horton[14] in 11-ODE system.

The further evolution of the system is possible only when parameters are changed. The most natural such change is to increase q. As soon as it crosses the threshold $q=q_*$, the T-state becomes unstable [see. Eq. (32)]. As we found in the previous subsection, this fixed point undergoes a Hopf bifurcation into a limit cycle that grows with growing criticality parameter $q-q_*>0$. At small $q-q_*>0$, the limit cycle oscillations are nearly linear in character, similar to the decaying oscillations at the final stage the T-mode relaxation dynamics, shown in Fig. 2. However, even a slight increase of q gives rise to the strong nonlinear oscillations, in which the zonal flow activity comes in bursts (Fig. 3). Each burst of the zonal flow causes strong suppression of the drift wave activ-

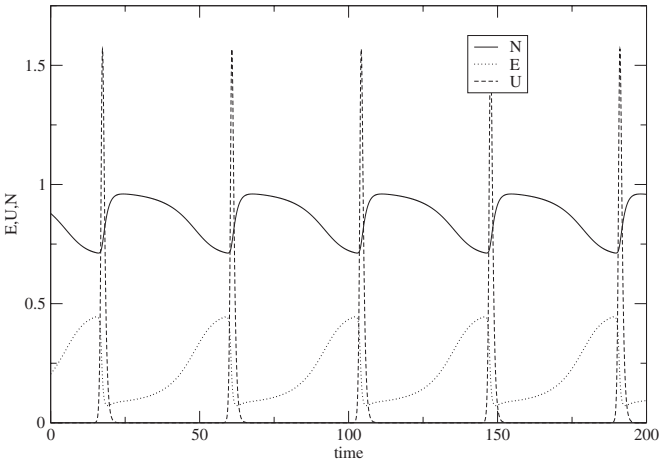

FIG. 3. Developed limit cycle oscillations around the oscillatory transient fixed point prior to the transition to the QH-mode, $q \approx 0.58$.

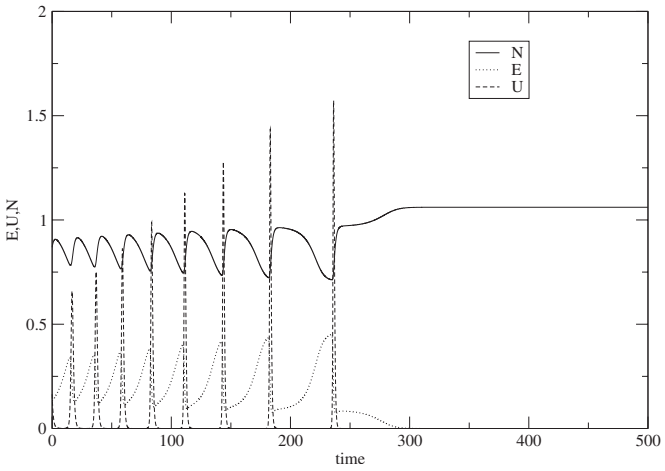

FIG. 4. Destruction of the limit cycle and transition to the QH-mode fixed point at $q \approx 0.582$.

ity and, as a result, significant increase of the temperature gradient N.

Finally, after some small increase of q up to $q=q_{\mathrm{crit}} \approx 0.582$, the limit cycle disappears and the orbit attracts to the QH-mode fixed point (Fig. 4). Note that the transition itself is preceded by the strongest zonal flow burst, strong enough to damp the drift wave turbulence completely, thus facilitating the transition to the QH-mode.

It should be emphasized that the above critical value of the control parameter q arises at the transition to the QH-mode from the vicinity of the T-mode, or more precisely from the local center manifold associated with the T-mode fixed point (e.g., the limit cycle). One can find other initial conditions that are away from the basin of attraction of the T-mode fixed point and the system will transit to the QH-mode for smaller values of q, down to approximately $q \simeq 0.54$. This will be discussed in more detail below.

A. Hysteresis

After the conditions for the forward transition from T- to QH-mode have been determined, the question whether the inverse transition occurs at the same value of the control parameter q is in order. The answer to this question essentially depends on how close to the QH fixed point the initial conditions are set. This is similar to the forward transition described earlier. For initial conditions set no farther than δN, δU, and $\delta E \sim 0.01$ from the QH-mode fixed point, the inverse transition to the T-mode fixed point can be delayed in the heating parameter q down to $q \simeq 0.55$, which is the stability boundary for the current set of parameters [Eq. (23)]. If, however, the trajectory of the system starts farther away from the QH-fixed point, it attracts to the T-mode for progressively higher values of q, which tends to the instability threshold of the limit cycle around the T-mode fixed point. This makes the hysteresis phenomenon not well pronounced. An accurate determination of the basin of attraction of the QH-mode fixed point for subcritical values of $q < q_{\mathrm{crit}} \approx 0.582$ is beyond the scope of this paper. It appears, however, that the role of hysteresis in the T→QH-mode transition is not very important. The reason for that is the following. Although there is a region of bistability

$$0.55 < q < 0.58,$$

where both the T-mode and the QH-mode are stable, the basins of attraction to these fixed points seem to be limited to the respective local center manifolds. Besides that, the interval of bistability (i.e., hysteresis) is less than 10% of the critical value of the control parameter q.

The above discussion is illustrated in Fig. 5, where four trajectories are shown for $q \simeq 0.56$; i.e., well inside of the bistability range. The first thing to notice is that the H-mode fixed point separates trajectories tending to the T-mode from those eventually making their way to the QH-mode. These two kinds of trajectories are marked in Fig. 5 as 2,4 and 1,3, respectively. It is clear that the orbits 1,2 and 3,4 run close together on the opposite sides of the H-mode stable manifold (separatrix) and then diverge along the unstable manifold and are ultimately attracted to the QH- and T-mode singular points, respectively. Therefore, *the hysteresis is sensitive to the initial conditions and not robust*.

It is important to emphasize that the forward and back transitions to the QH-mode are not symmetric, even though the hysteresis is not well pronounced. The fundamental asymmetry is in that the forward transition from a stable L-state proceeds, as the power input q increases to the stable QH-state through the oscillatory, intermediate T-mode, so that the system goes out of the $U=0$ plane. The back transition QH→L typically occurs on the $U=0$; i.e., without ZF excitation. This property of the system is demonstrated in Fig. 6.

B. Stabilization of the QH-mode fixed point

Apart from the hysteresis described above, the QH-mode can be stabilized at a subcritical heating level by applying modulated rather than constant heating rate q. We illustrate the stabilization phenomenon in Fig. 7. In addition to the constant $q=\bar{q}=0.54$ [which corresponds to a slightly unstable QH-mode, Eq. (23)] we add the modulated part $\tilde{q}=0.08$. The QH-mode then sustains for about 150 dimensionless time

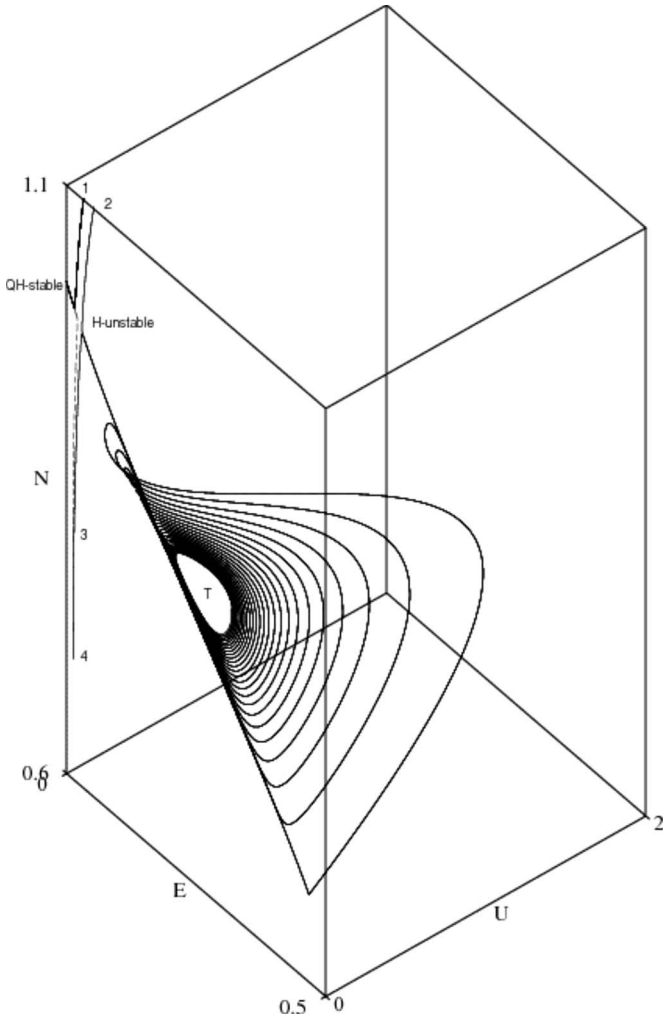

FIG. 5. Three-dimensional trajectories, shown for the following set of initial conditions $N=1.1, 0.7, 0.8$; $U=0.01$ (in all three cases); $E=0.01, 0.03, 0.05$. Other parameters are fixed at the same values as in Fig. 1.

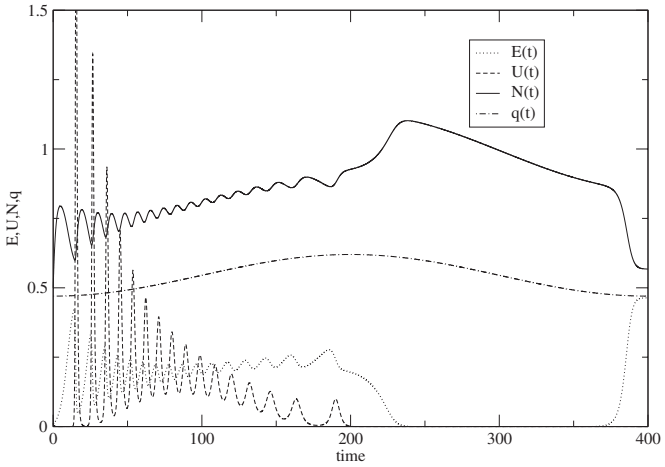

FIG. 6. Sequence of transitions shown for $q(t)$ slowly varying from $q=0.47$ (stable L-mode condition) to $q=0.62$ (stable QH) and back. Other parameters are the same as in Fig. 1.

units, as opposed to the runs with $\tilde{q}=0$, where the QH-mode quickly decays to the T-mode going through the metastable states near the H- and L-modes (Fig. 2).

V. SUMMARY AND CONCLUSIONS

In this paper we have investigated a low order (3-ODE) model of L-H transition formulated earlier in Refs. 25 and 26. Particular emphasis has been made on the study of the oscillatory transient mode which appears to be a key for understanding the dynamics of the L-H transition.

The principal results of this study are:

(1) There are as many as four stationary states of the system (singular points of ODEs) which can be organized by growing pressure gradient (and generally by the increasing control parameter q) in the following manner: L-mode, transient oscillatory T-mode, H-mode, and, finally, the quiescent H-mode (QH). Physically, their meaning is as follows. In the L-mode, the DW instability driven by the pressure gradient saturates due to the nonlinearity of the DW mode and due to the mean flow. The ZF is not active. With the increasing power the T-mode is activated in which the ZF is generated and provides an additional suppression of the DW which, in turn, drives ZF. This feedback loop naturally results in an oscillatory behavior of the T-mode, which can be attributed to the dithering observed in various experiments on the L-H transition.[18] In the H-mode, the ZF is again suppressed completely as in L-mode, but the pressure gradient is higher because of the multiplicity of the DW stationary states, caused by their nonlinear pressure gradient dependence. In the QH-mode, not only the ZF but also the DW vanishes completely and the heat production is balanced by the neoclassical transport.

(2) We identified *center manifolds* of these fixed points. These are two-dimensional attractors which the system orbits quickly approach when they are close to the cor-

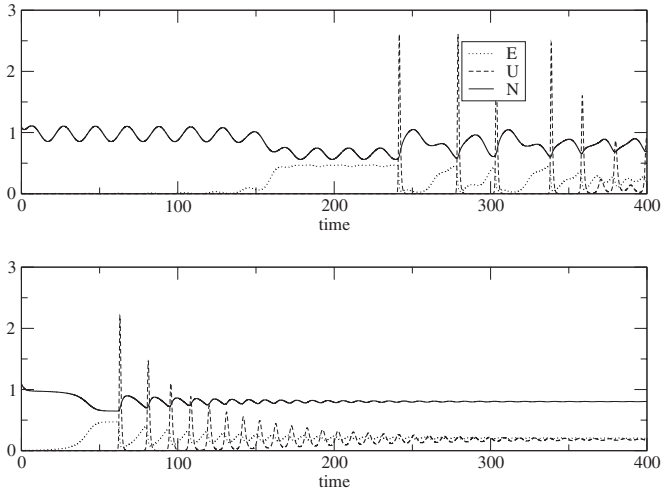

FIG. 7. Stabilization of the QH-mode by the modulation of heating rate q. The upper panel shows a numerical solution with the average $\bar{q}=0.54$, the oscillatory part $\tilde{q}=0.08$, and the modulation frequency $\omega=0.31$. The initial conditions are chosen close to the QH-mode with $U=E=0.01$. The lower panel shows the run with $\tilde{q}=0$ and for the same values of the remaining parameters.

responding fixed points. The further dynamics unfolds essentially on these center manifolds.

(3) The center manifold associated with the L,H and QH equilibria is simply the $U=0$ plane (zero zonal flow intensity), while on the T-mode center manifold all the three variables are active. The T-mode is a stable focus that undergoes Hopf bifurcation to a stable limit cycle when $q>q_*$. When q increases further, $q>q_{\mathrm{crit}}$, the limit cycle solution is destroyed, and the system proceeds to the QH-mode. While the T-mode center manifold does not coincide with any coordinate plane of the three variables, it is still *two dimensional* and therefore the dynamical chaos is absent. This fact was not revealed from more detailed previous models with large numbers of equations (see, e.g., Ref. 14).

(4) There is a parameter range of bistability where both the T- and QH-modes coexist and are stable (or the stable limit cycle around T-mode exists) which underpins hysteresis. The hysteresis range is relatively narrow, less than 10% of q_{crit}.

(5) The L mode is a stable node on the $U=0$ center manifold, while the H-mode is a hyperbolic fixed point on this manifold. The latter fixed point has thus a stable invariant manifold (branch of a separatrix), but being hyperbolic is unstable in general. However, a distinct metastable state at the H-mode, that persists for a few hundred dimensionless time units, is identified. The L-mode, when unstable with respect to the zonal flow generation, also constitutes a strong attractor on the $U=0$ manifold. The corresponding metastable state can last for more than 100 time units before it leaves the $U=0$ manifold and transits to the T-mode.

(6) Transition from L-mode to higher stable confinement modes (T or QH) cannot be made without zonal flow generation, even though zonal flow eventually dies out when the system reaches the QH-mode. Physically, the T-mode occurs when the system is powered at an intermediate rate (between the L- and QH-modes) and cannot be overridden at the ramp-up stage.

(7) However, the reverse QH→L transition is not symmetric with the forward transition in that it can occur without ZF generation, which is also indicative of hysteresis (see Ref. 4).

The above results allow one to describe time-dependent L→H transition including quiescent H-mode and the oscillatory transient mode. The three-dimensional dynamical system utilized in this paper is clearly the minimal one to feature these aspects of the transport bifurcation. On the other hand, it is simple enough to allow one to construct the two-dimensional center manifolds near the respective singular points of the system, to study their structure, and to estimate the strength of hysteresis associated with the transition. In particular, bursting and dithering are interpreted by standard means of the theory of dynamical systems as a limit cycle on the center manifold near the transient oscillatory (T) fixed point. In addition, it is demonstrated mathematically that the zonal flow excitation is a necessary step in a transition to an improved confinement mode, even though the latter may ultimately eliminate the zonal flow.

ACKNOWLEDGMENTS

This research was supported by Department of Energy, Grant No. DE-FG02-04ER54738.

[1] F. Wagner, G. Becker, K. Behringer, D. Campbell, A. Eberhagen, W. Engelhardt, G. Fussmann, O. Gehre, J. Gernhardt, G. V. Gierke, G. Haas, M. Huang, F. Karger, M. Keilhacker, O. Klüber, M. Kornherr, K. Lackner, G. Lisitano, G. G. Lister, H. M. Mayer, D. Meisel, E. R. Müller, H. Murmann, H. Niedermeyer, W. Poschenrieder, H. Rapp, H. Röhr, F. Schneider, G. Siller, E. Speth, A. Stäbler, K. H. Steuer, G. Venus, O. Vollmer, and Z. Yü, Phys. Rev. Lett. **49**, 1408 (1982).
[2] W. Horton, Rev. Mod. Phys. **71**, 735 (1999).
[3] J. W. Connor and H. R. Wilson, Plasma Phys. Controlled Fusion **42**, 1 (2000).
[4] P. W. Terry, Rev. Mod. Phys. **72**, 109 (2000).
[5] R. A. Moyer, G. R. Tynan, C. Holland, and M. J. Burin, Phys. Rev. Lett. **87**, 135001 (2001).
[6] P. H. Diamond, S.-I. Itoh, K. Itoh, and T. S. Hahm, Plasma Phys. Controlled Fusion **47**, 35 (2005).
[7] B. N. Rogers, J. F. Drake, and A. Zeiler, Phys. Rev. Lett. **81**, 4396 (1998).
[8] Z. Lin, T. S. Hahm, W. W. Lee, W. M. Tang, and P. H. Diamond, Phys. Rev. Lett. **83**, 3645 (1999).
[9] P. Beyer, S. Benkadda, X. Garbet, and P. H. Diamond, Phys. Rev. Lett. **85**, 4892 (2000).
[10] A. M. Dimits, G. Bateman, M. A. Beer, B. I. Cohen, W. Dorland, G. W. Hammett, C. Kim, J. E. Kinsey, M. Kotschenreuther, A. H. Kritz, L. L. Lao, J. Mandrekas, W. M. Nevins, S. E. Parker, A. J. Redd, D. E. Shumaker, R. Sydora, and J. Weiland, Phys. Plasmas **7**, 969 (2000).
[11] P. Beyer, S. Benkadda, G. Fuhr-Chaudier, X. Garbet, P. Ghendrih, and Y. Sarazin, Phys. Rev. Lett. **94**, 105001 (2005).
[12] X. Garbet, Fusion Sci. Technol. **53**, 348 (2008).
[13] C. S. Chang, S. Klasky, J. Cummings, R. Samtaney, A. Shoshani, L. Sugiyama, D. Keyes, S. Ku, G. Park, S. Parker, N. Podhorszki, H. Strauss, H. Abbasi, M. Adams, R. Barreto, G. Bateman, K. Bennett, Y. Chen, E. D'Azevedo, C. Docan, S. Ethier, E. Feibush, L. Greengard, T. Hahm, F. Hinton, C. Jin, A. Khan, A. Kritz, P. Krsti, T. Lao, W. Lee, Z. Lin, J. Lofstead, P. Mouallem, M. Nagappan, A. Pankin, M. Parashar, M. Pindzola, C. Reinhold, D. Schultz, K. Schwan, D. Silver, A. Sim, D. Stotler, M. Vouk, M. Wolf, H. Weitzner, P. Worley, Y. Xiao, E. Yoon, and D. Zorin, Inst. Phys. Conf. Ser. **125**, 012042 (2008).
[14] G. Hu and W. Horton, Phys. Plasmas **4**, 3262 (1997).
[15] L. Chen, Z. Lin, and R. White, Phys. Plasmas **7**, 3129 (2000).
[16] R. J. Groebner, K. H. Burrell, and R. P. Seraydarian, Phys. Rev. Lett. **64**, 3015 (1990).
[17] R. A. Moyer, K. H. Burrell, T. N. Carlstrom, S. Coda, R. W. Conn, E. J. Doyle, P. Gohil, R. J. Groebner, J. Kim, R. Lehmer, W. A. Peebles, M. Porkolab, C. L. Rettig, T. L. Rhodes, and R. P. Seraydarian, Phys. Plasmas **2**, 2397 (1995).
[18] K. H. Burrell, Phys. Plasmas **4**, 1499 (1997).
[19] D. E. Newman, B. A. Carreras, D. Lopez-Bruna, P. H. Diamond, and V. B. Lebedev, Phys. Plasmas **5**, 938 (1998).
[20] P. H. Diamond, S. Champeaux, M. Malkov, A. Das, I. Gruzinov, M. N. Rosenbluth, C. Holland, B. Wecht, A. I. Smolyakov, F. L. Hinton, Z. Lin, and T. S. Hahm, Nucl. Fusion **41**, 1067 (2001).
[21] Z. N. Andrushchenko and V. P. Pavlenko, Phys. Plasmas **9**, 4512 (2002).
[22] G. R. McKee, R. J. Fonck, M. Jakubowski, K. H. Burrell, K. Hallatschek, R. A. Moyer, D. L. Rudakov, W. Nevins, G. D. Porter, P. Schoch, and X. Xu, Phys. Plasmas **10**, 1712 (2003).
[23] M. G. Shats, W. M. Solomon, and H. Xia, Phys. Rev. Lett. **90**, 125002 (2003).
[24] P. Gohil, G. R. McKee, D. Schlossberg, L. Schmitz, and G. Wang, Inst. Phys. Conf. Ser. **123**, 012017 (2008).
[25] E.-J. Kim and P. H. Diamond, Phys. Rev. Lett. **90**, 185006 (2003).
[26] E.-J. Kim and P. H. Diamond, Phys. Plasmas **10**, 1698 (2003).
[27] H. Zohm, Phys. Rev. Lett. **72**, 222 (1994).
[28] H. Sugama and W. Horton, Plasma Phys. Controlled Fusion **37**, 345 (1995).
[29] M. A. Malkov, P. H. Diamond, and M. N. Rosenbluth, Phys. Plasmas **8**, 5073 (2001).

[30]V. S. Marchenko, Phys. Rev. Lett. **89**, 185002 (2002).
[31]O. E. Garcia and N. H. Bian, Phys. Rev. E **68**, 047301 (2003).
[32]J.-N. Leboeuf, L. A. Charlton, and B. A. Carreras, Phys. Fluids B **5**, 2959 (1993).
[33]R. J. Colchin, M. J. Schaffer, B. A. Carreras, G. R. McKee, R. Maingi, T. N. Carlstrom, D. L. Rudakov, C. M. Greenfield, T. L. Rhodes, E. J. Doyle, N. H. Brooks, and M. E. Austin, Phys. Rev. Lett. **88**, 255002 (2002).
[34]N. H. Bian and O. E. Garcia, Phys. Plasmas **10**, 4696 (2003).
[35]B. A. Carreras, D. Newman, P. H. Diamond, and Y.-M. Liang, Phys. Plasmas **1**, 4014 (1994).
[36]P. H. Diamond, V. B. Lebedev, D. E. Newman, and B. A. Carreras, Phys. Plasmas **2**, 3685 (1995).
[37]W. Horton, G. Hu, and G. Laval, Phys. Plasmas **3**, 2912 (1996).
[38]K. Itoh, S.-I. Itoh, P. H. Diamond, T. S. Hahm, A. Fujisawa, G. R. Tynan, M. Yagi, and Y. Nagashima, Phys. Plasmas **13**, 055502 (2006).
[39]K. Miki, Y. Kishimoto, J. Li, and N. Miyato, Phys. Plasmas **15**, 052309 (2008).
[40]P. H. Diamond, Y.-M. Liang, B. A. Carreras, and P. W. Terry, Phys. Rev. Lett. **72**, 2565 (1994).